1444–1449 Nucleic Acids Research, 1994, Vol. 22, No. 8

Theoretical studies of DNA – RNA hybrid conformations

Sanjay R.Sanghani and Richard Lavery*
Laboratoire de Biochimie Théorique, CNRS URA 77, Institut de Biologie Physico-Chimique, 13 rue Pierre et Marie Curie, Paris 75005, France

Received December 20, 1993; Revised and Accepted March 21, 1994

ABSTRACT

Molecular modelling has been used to probe the conformational preferences of double stranded DNA – RNA hybrids. As might be expected, the sugars of the DNA strand have higher conformational flexibility, but, for the majority of the repetitive sequences studied, these sugars prefer a $C_{2'}$-endo pucker, while ribose sugars uniformly adopt a $C_{3'}$-endo pucker. This gives rise to a strongly heteronomous duplex conformation. One exception to this rule involves the thymidine strand of poly(dT).poly(rA), which marginally prefers a $C_{3'}$-endo pucker. Our study further indicates that the DNA strands of the hybrids favour backbone torsions in the canonical B domain, rather than the modified values proposed on the basis of fibre diffraction studies. Backbone conformational transitions can nevertheless be induced leading to an $\alpha\gamma$-flip (α:γ, $g^-/g^+ \rightarrow t/t$) or to the $\alpha\beta\gamma$-flip form proposed from fibre studies (α:β:γ, $g^-/t/g^+ \rightarrow t/g^+/t$). The latter transition is also found to be linked to $B_I \rightarrow B_{II}$ transitions (ϵ:ζ, $t/g^- \rightarrow g^-/t$).

INTRODUCTION

Double stranded DNA–RNA hybrids play key roles in a wide variety of biological information transfer processes. Notably, they act as primers during DNA replication in the form of Okazaki fragments, they are intermediates in the reverse transcription of retroviral RNA and in the transcription of DNA into messenger RNA. However, the conformational properties of such hybrids have been much less studied than those of more usual DNA duplexes, in part due to difficulties in synthesising pure RNA oligomers in significant quantities (1,2). The first information concerning the secondary structure of DNA–RNA hybrids was obtained from fibre diffraction experiments on DNA from the fd phage associated with its transcribed RNA (3). The authors of this study suggested that the corresponding diffraction patterns were not indicative of a B conformation and it was commonly assumed that the strong preference of RNA strands to adopt the A conformation would probably force this conformation on hybrid duplexes. The first study providing evidence contrary to this assumption was presented by Gray and Ratliff in 1975 (4). Their investigation of the circular dichroism of poly(dAC).poly (rGU) and poly(dGT).poly(rAC) indicated conformations intermediate between those of pure DNA and RNA duplexes. However, upon reduction of the relative humidity of the samples, both spectra tended towards that of the canonical RNA duplex.

In 1981, Zimmerman and Pheiffer (5) showed that fibres of the homopolymeric hybrid poly(dT).poly(rA) could adopt two distinct conformations depending upon their relative humidity. At low relative humidity, an A conformation was found, with all sugars adopting $C_{3'}$-endo puckers. At high relative humidity, a heteronomous conformation resulted, having B-like $C_{2'}$-endo sugars within the DNA strand and A-like $C_{3'}$-endo sugars within the RNA strand. Later ^{31}P nuclear magnetic resonance studies of the same hybrid (6) were in good agreement with the fibre diffraction models in that a conformational transition was observed around 90% relative humidity. Further fibre studies from Arnott's group also proposed heteronomous conformations for the homopolymer hybrids poly(dA).poly(rU) and poly(dI).poly(rC) (7). More recently, high resolution 2D NMR studies (8), have shown that the hybrid oligomer d(CGTTATA-ATGCG).r(CGCAUUAUAACG) also adopts a heteronomous secondary structure, with $C_{3'}$-endo sugars in the RNA strand, and less clearly defined S-domain puckers in the DNA strand. Similar conclusions were reached in a study of the hybrid oligomer d(GTCACATG).r(CAUGUGAC) (9).

Recent theoretical work from our laboratory (10) using the Jumna algorithm, has indicated that B-DNA with regular repeating sequences is commonly associated with a number of conformational sub-states belonging to the B-family. These sub-states generally have similar stabilities, although their conformations can differ significantly. It has been found that these sub-states could be characterised by their sugar puckering, which in turn was linked to many other features of local helicoidal conformation. In contrast, studies of A-DNA showed no such multiplicity of sub-states (11). In the present study we apply similar techniques to an investigation of the conformational properties of DNA–RNA hybrids. We take into account the effects of base sequence and also study a certain number of conformational transitions involving backbone dihedral angles.

METHODOLOGY

Details of the Jumna algorithm (Junction Minimisation of Nucleic Acids) and its associated Flex force field have been presented elsewhere (12–15). Jumna models the flexibility of the nucleic acid fragments, by a combination of helicoidal and internal

*To whom correspondence should be addressed

variables. Helicoidal variables determine the position of each nucleotide (3'-monophosphate) with respect to a common helical axis system, while single bond rotations at the glycosidic bond and within the phosphodiester backbone and valence angles within the sugar rings describe internal nucleotide conformations. Harmonic constraints are used to ensure the closure of sugar rings and of backbone linkages between nucleotides during energy minimisation.

There are several advantages of working within a framework of helicoidal parameters. Firstly, the number of degrees of freedom needed to model a nucleic acid fragment is approximately one tenth of those needed in classical Cartesian molecular mechanics. Secondly, this choice facilitates the imposition of helical symmetry by simply making appropriate sets of parameters identical to each other. If such symmetry is appropriate for the problem in hand, a further reduction in the number of degrees of freedom can be achieved. Direct use of internal and helicoidal coordinates also allow many features of nucleic acid conformation to be controlled during the course of an energy minimisation. One example of this involves fixing desired values for sugar phase angles, which can be achieved using a quadratic penalty function of the difference between the actual and the desired phase angles. These phases can be translated via the standard pseudorotation formula (16) into forces which act on the atoms of the sugar ring and generate the necessary ring dihedral angles. Directly controlling sugar pucker turns out to be a very effective way of passing between different nucleic acid conformations (17). The current version of the Jumna program (version 7.2) is provided with an new option for automatically producing 1- and 2-dimensional adiabatic maps along chosen vectors or within chosen planes of conformational space. This option is put to use in the present study for locating energy minima and determining pathways between different conformational states.

It should be stressed that although Jumna does not model changes in bond lengths or in valence angles (other than those associated with the sugar rings), this does not prevent the detection of fine base sequence effects on nucleic acid conformation. The experience we have gained in treating both static conformations and transitions pathways (17,18) suggests that the increased ease of minimisation using Jumna more than compensates for the loss of the stiffer degrees of freedom.

Since all calculations presented here involve regular repeating base sequences it is preferable to model infinite, symmetric polymers rather than irregular oligomers, where end-effects can confuse underlying sequence effects. Jumna simulations were therefore carried out with helical symmetry constraints. Conformational energies are presented as energies per repeating unit (Ecen), this unit consisting of either 1 or 2 nucleotide pairs depending on whether mono or dinucleotide symmetry is imposed. Interactions of the central repeating unit with 9 nucleotide pairs on either side are taken into account and end-effects can therefore be considered to be absent. As in earlier studies (10,17), solvent dielectric damping was taken into account via a sigmoidal dielectric function (12,19) and the net phosphate charges were reduced to −0.5e (+0.25e being added to each anionic oxygen) to mimic the effect of counterion binding.

RESULTS AND DISCUSSION

The four possible homopolymer DNA−RNA hybrids poly(dT).poly(rA), poly(dA).poly(rU), poly(dG).poly(rC) and poly(dC).poly(rG) were energy minimized while imposing

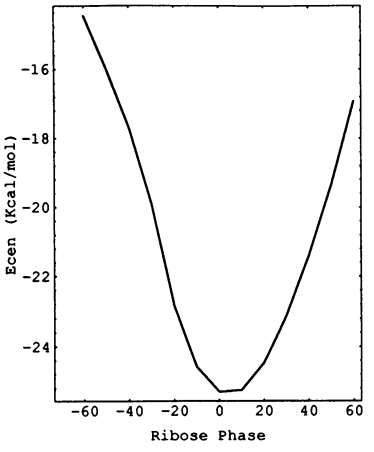

Figure 1. Conformational energy (kcal/mol) of dT.rA, constrained to mononucleotide symmetry, as a function of: ribose sugar phase.

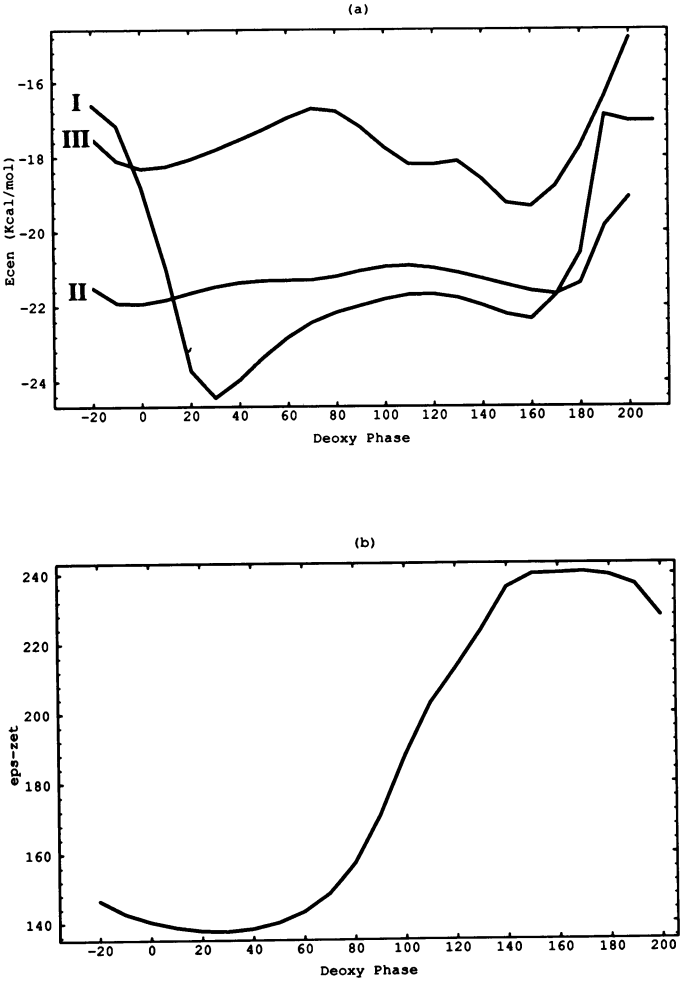

Figure 2. (a) Conformational energy (kcal/mol) of dT.rA models as a function of deoxyribose sugar phase: I. with the most stable backbone conformation ($\alpha\beta\gamma$: $g^-/t/g^+$), II, with an $\alpha\gamma$ flip ($\alpha\beta\gamma$: t/t/t), III. with an $\alpha\beta\gamma$ flip ($\alpha\beta\gamma$: $t/g^+/t$). (b) $B_I \rightarrow B_{II}$ transition provoked by decreasing sugar phase for the dT.rA model with an $\alpha\beta\gamma$ flip.

mononucleotide symmetry. For each of these homopolymers, the energy per repeating unit was calculated as a function of deoxyribose sugar pucker for values ranging from $C_{3'}$-endo to $C_{2'}$-endo (corresponding to phases ranging from roughly 0° to 180°). In view of recent computations which indicated that the most stable form of the DNA duplex poly(dA).poly(dT) exhibited a dinucleotide repeat (20), the homopolymer DNA−RNA hybrid calculations were also performed with dinucleotide symmetry constraints. In order to cover the full range of dinucleotide sequences, these calculations were completed by studies of the alternating sequence hybrids poly(dAC).poly(rGU), poly(dTG).poly(rCA), poly(TA).poly(rUA), poly(dCG).poly(rCG), poly(dAG).poly(rCU) and poly(dTC).poly(rGA) using dinucleotide symmetry constraints.

The conformational complexity of the systems to be investigated was reduced by noting that the ribose sugars remained steadfastly around the $C_{3'}$-endo pucker, as has frequently been observed experimentally for helical RNA's (21). Figure 1 shows the dependence of Ecen upon the phase angle of the ribose sugars of poly(dT).poly(rA) (abbreviated hereafter as dT.rA), under mononucleotide symmetry. The resulting sharp energy minimum centred on the $C_{3'}$-endo pucker is typical of all the ribose sugars in the hybrid polymers studied. This may be contrasted, in figure 2, with the relative ease of modifying the deoxyribose between $C_{3'}$-endo and $C_{2'}$-endo forms. Sugar pucker flexibility in DNA−RNA duplexes thus appears to be limited largely to the deoxyribose strand and consequently studying repuckering effects in homopolymers under mononucleotide symmetry becomes a one constraint problem. By a similar rational, the study of alternating sequences (or homopolymers) under dinucleotide symmetry will be a two constraint problem; one constraint being applied to each symmetry distinct deoxyribose sugar. (It should be noted however that although only deoxyribose phase angles are controlled in the mapping described below, ribose phase angles are free vary, as are all other degrees of freedom within the nucleic acid polymers studied).

Table 1. Conformational energies per repeating unit (kcal/mol) for homopolymer hybrids with imposed mononucleotidic symmetry

Sequence	A form	B form	ΔE (B−A)	ΔEact.
dG.rC	−38.8	−41.0	−2.2	3.6
dC.rG	−40.4	−41.5	−1.1	2.5
dA.rU	−24.2	−24.5	−0.3	2.3
dT.rA	−24.4	−22.4	2.0	2.7
dT.rA (with αβγ flip)	−18.3	−19.3	−1.0	2.6
dT.rA (with αγ flip)	−21.9	−21.7	0.2	0.9

ΔEact. corresponds to the calculated activation energy necessary escape from the most stable state.

As discussed in the introduction, various conformations have been proposed for DNA−RNA hybrids. These models share the feature that the DNA strand seems to behave in a polymorphic manner, adopting either B or A conformations as a function of sequence and environment. For a given homopolymer, we have found that the transition from A to B form within the deoxyribose strand occurs with no significant change in structure for the ribose strand. The base pairs constituting the hybrid double helix are therefore sufficiently flexible to allow these effects. Such decoupling of the two strands within a duplex structure has also been observed in the case of pure DNA duplexes (20). Table 1 gives the conformational energies of the two stable forms located for each of the homopolymer sequences. Since continuous adiabatic mapping of sugar phase angle was used to locate these two energy minima, it is also possible to determine the energy barrier separating these forms. These values cover a range of roughly 2 → 4 kcal/mol. With the exception of the hybrid dT.rA, the DNA strand is most stable with $C_{2'}$-endo sugars.

For dT.rA, three distinct states could be found which persisted for all deoxyribose sugar puckers (figure 1). These states were distinguished by the α (O3'-P-O5'-C5'), β (P-O5'-C5'-C4') and γ (O5'-C5'-C4'-C3') backbone dihedrals which adopted either the $g^-/t/g^+$ conformation found in both canonical A- and B-DNA, changes of α and γ to trans (which we will term an αγ flip), or changes of α, β and γ to α $t/g^+/t$ conformation (hereafter termed an αβγ flip). The latter backbone conformation corresponds to that proposed by Zimmerman and Pheiffer using fibre diffraction (5). The αβγ flip leads to a preference for C2'-endo sugars within the DNA strand for all the base sequences investigated as well as a certain number of changes in helicoidal parameters. These involve a decrease in Xdisp (more negative by 1Å → 4.4Å, with the exception of the B form of dT.rA where it was 0.3Å more positive). Twist also decreased significantly for the dA.rU and dC.rG (3.7° → 6.5°), but was almost unaffected for the other sequences. Rise decreased for dT.rA and dG.rC (0.2Å → 0.5Å), but increased for the remaining sequences. It should be remarked that conformations involving αγ flips have been observed crystallographically and Heinemann and co-workers (22) have suggested that such transitions facilitate

Table 2. Comparison of calculated and experimental torsion angles for dT.rA and dA.rU

Strand	Conformation	α	β	ζ	δ	ε	γ
DNA	dT.rA model	297	176	251	134	187	56
	dT.rA model (αβγ flip)	208	87	322	141	202	162
	dT.rA fibre (ref. 5)	180	96	324	152	182	166
	dA.rU model	294	181	244	145	189	53
	dA.rU fibre (ref. 7)	291	184	259	130	186	51
RNA	dT.rA model	279	174	283	92	207	67
	dT.rA model (αβγ flip)	276	175	284	94	210	66
	dT.rA fibre (ref. 5)	272	174	283	97	214	75
	dA.rU model	277	170	296	84	201	74
	dA.rU fibre (ref. 7)	284	180	288	84	207	60

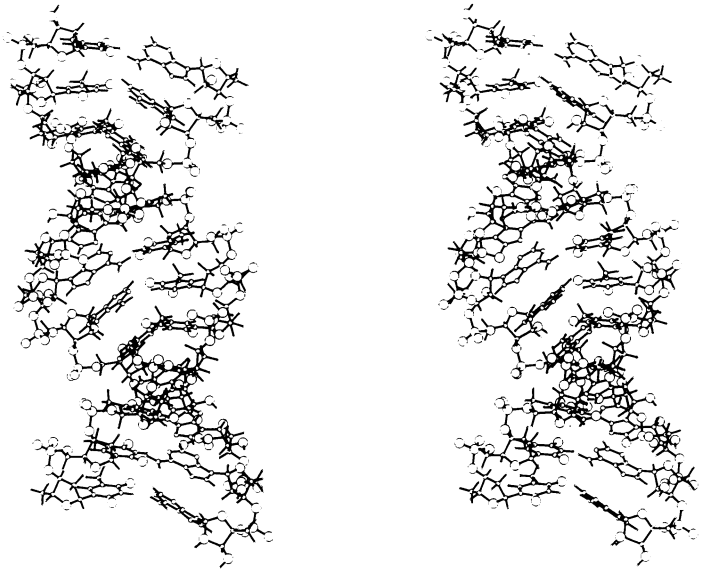

Figure 3. Stereoscopic diagram of dT.rA in its most stable conformation.

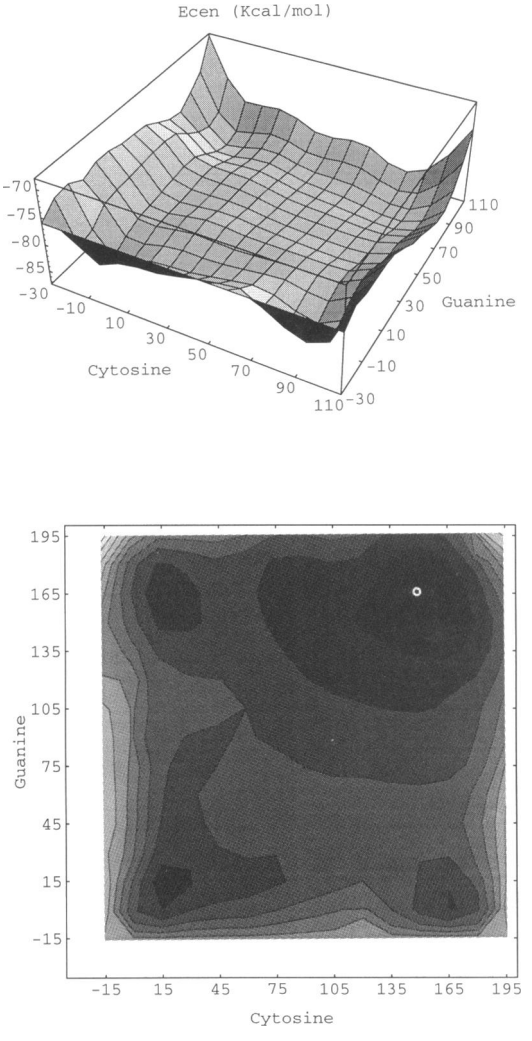

Figure 4. 3D-conformational energy surface and corresponding contour plot for dCG.rCG as a function of the cytidine and guanidine sugar phase angles within the DNA strand.

greater intrastrand stacking. An apparent anti-correlation between the values of α and γ has also been pointed out (23).

Table 2 compares the backbone torsion angles of the DNA and RNA strands in our models with those of the Zimmerman and Pheiffer and also of Arnott. A close agreement is seen in the case of the model with the $\alpha\beta\gamma$ flip. In contrast, the backbone with canonical α, β and γ dihedrals corresponds to the conformations of the other homopolymers studied and to the fibre model proposed for dA.rU (7) with the exception of a change in the phase angle of the deoxyribose sugars which leads to a difference in the backbone dihedral δ. As the data in figure 2 and table 1 show, the state without the $\alpha\gamma$ or $\alpha\beta\gamma$ flips is in fact more stable for almost the full range of the deoxyribose pucker values studied. This finding is supported by recent 2D NMR studies (9). Figure 3 shows a stereo plot of the most stable dT.rA structure. An intra-strand hydrogen bond within the RNA strand (between a ribose O2′-hydroxyl group and the 3′-ribose O4′, 3.0Å) which has been noted experimentally, is also evident in this model. This conformation exhibits an important base pair buckle and a large propeller, often seen with AT pairs. It nevertheless maintains good hydrogen bonding within each base pair.

When an $\alpha\beta\gamma$ flip is present, it actually results in a further backbone transition as the deoxyribose phase angle is decreased. As figure 2 shows, this change involves a smooth B_I to B_{II} transition (24, 25) corresponding to a change in the difference $\epsilon-\zeta$ (C4′-C3′-O3′-P and C3′-O3′-P-O5′ respectively) from roughly $-100°$ to $+100°$ ($tg^- \rightarrow g^-t$). It may also be remarked that this transition is essential to maintaining the $\alpha\beta\gamma$ flip in dT.rA with a A-form of the DNA strand. If a B_I conformation is enforced then the values of α, β and γ return to their canonical values. Similar transitions in the A-form of the DNA strand were also observed with dinucleotide sequences upon which the $\alpha\beta\gamma$ flip was imposed.

Concerning the $\alpha\gamma$ flip, it is remarked that the RNA strand of the hybrids may also undergo the $\alpha\gamma$ flip (as observed experimentally in certain RNA duplexes, 26), but as for the DNA strand, this change always led to less stable structures and will not be discussed further.

When dinucleotide symmetry was allowed to develop in the homopolymers, all conserved mononucleotide conformations with the exception of dA.rU. This polymer developed a dinucleotide conformation with successive sugar phases differing by roughly 20° and successive base pair twist angles differing by roughly 5°. This conformation was more stable by 0.3 kcal/mol. This change is analogous to the symmetry reduction observed earlier for the dA.dT duplex (20).

We now turn to the study of alternating base sequences. In this case, mapping all possible deoxyribose puckering requires a 2-dimensional energy surface. Such data is shown in figure 4 shows for the case of dCG.rCG, the two dimensions of the map corresponding to the sugar phases of guanidine and cytidine within the DNA strand. This map is typical of all the surfaces obtained for alternating base sequences under dinucleotide symmetry without $\alpha\gamma$ or $\alpha\beta\gamma$ flips. The global minimum is located at phase values corresponding to $C_{2'}$-endo for both

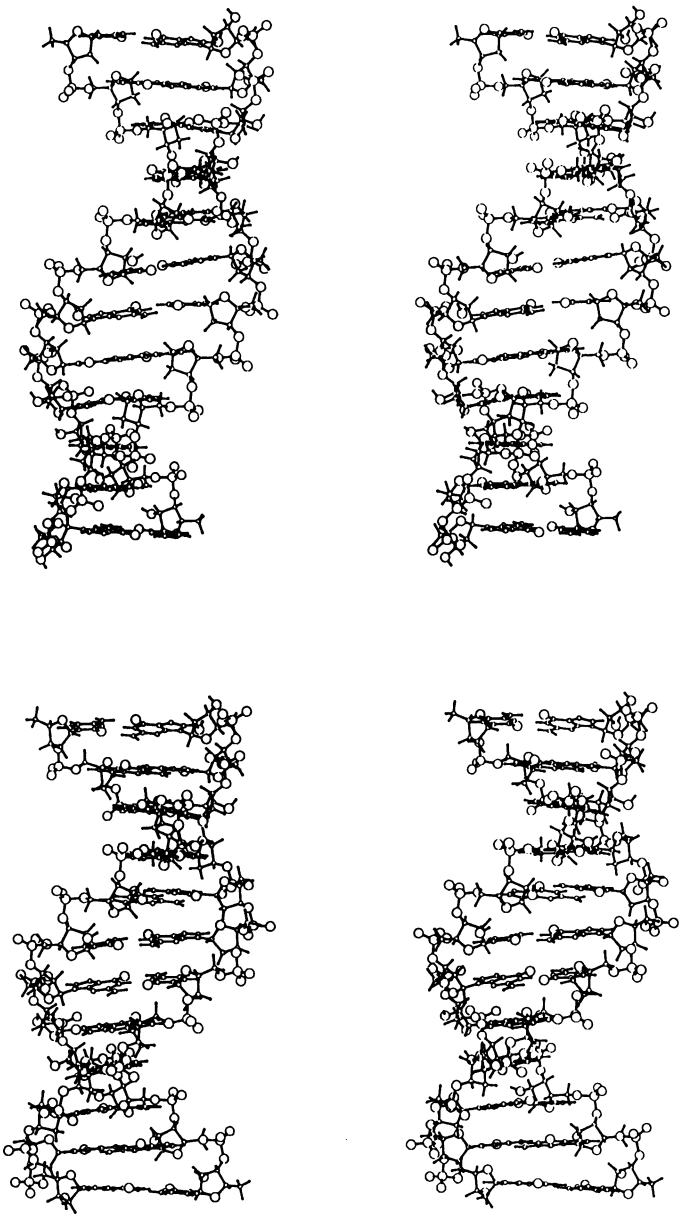

Figure 5. Stereoscopic diagrams of dCG.rCG. Top: DNA strand in the A conformation. Bottom: DNA strand in the B conformation.

Table 3. Conformational energy per repeating unit (kcal/mol) sugar pucker for alternating sequence hybrids with imposed dinucleotidic symmetry

Sequence	Nucleotide	Phase	Amplitude	Energy
dAC.rUG	A	154	43.6	−67.1
	C	167	34.2	
dCG.rCG	G	159	39.7	−87.2
	C	158	41.7	
dGA.rCU	G	148	43.2	−67.0
	A	158	38.6	
dTA.rAU	T	151	40.5	−50.2
	A	155	39.4	
dTC.rAG	T	155	42.4	−67.2
	C	156	39.0	
dTG.rAC	T	157	38.9	−66.9
	G	150	42.2	

Table 4. The resulting global minima after the imposition of an $\alpha\gamma$ flip, at various positions, on the dinucleotide sequences

RY	GT	S	N	YR	TG	N	N	All	GT	N	S
	GC	S	E		CG	S	N		GC	N	N
	AT	s	s		TA	N	N		AT	S	N
	AC	S	E		CA	N	N		AC	N	S
RR	GA	N	N	YY	TC	N	N	All	GA	N	S
	AG	N	N		CT	N	N	All	TC	N	S

Key: R=purine, Y=pyrimidine, S=C2′-endo, N=C3′-endo, E=O1′-endo, s=E/S. RY, YR, RR and YY indicate a flip is present at this type of step. 'All' indicates that flips are present at all steps.

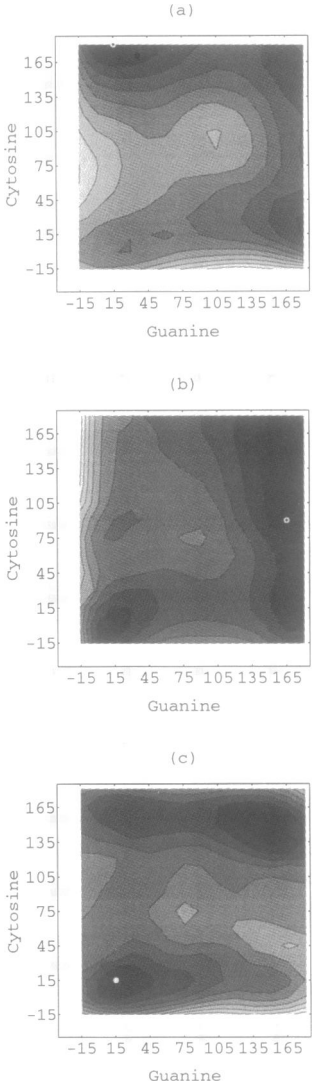

Figure 6. Conformational energy contour plots for dCG.rCG as a function of the cytidine and guanidine sugar phase angles within the DNA strand: (**a**) $\alpha\gamma$ flip at each dCdG step; (**b**) $\alpha\gamma$ flip at each dGdC; (**c**) $\alpha\gamma$ flip all dinucleotide steps in the DNA strand.

deoxyribonucleotides. Slightly less stable local minima are located in the remaining corners of the map, correspond to structures with mixed $C_{2'}$-endo/$C_{3'}$-endo sugar puckers or to pure $C_{3'}$-endo puckers within the deoxyribose strand. Moving from the global

minimum to any of these secondary minima results in a loss of 2–3 kcal/mol and requires passing energy barriers of roughly 1.5 kcal/mol. Figure 5 shows stereoscopic diagrams of dCG.rCG with its deoxyribose strand in both the A and B conformations. It is remarked that the occurrence of mixed puckers in duplex DNA has been the subject of several investigations (27, 28). Such states have been observed, for example with the alternating sequence dTA.dTA under low salt conditions. Table 3 lists the conformational energies and the deoxyribose sugar puckers for the most stable minima located for each sequence. Although all the DNA strand sugars adopt the $C_{2'}$-endo classification, the vast majority of them lie close to the $C_{1'}$-exo conformation with relatively low phase angles (8).

The introduction of an $\alpha\gamma$ flip with dinucleotide sequences generally resulted in a loss of stability of several kcal/mol, but also affected the relative stability of the minima discussed (see table 4). When the flip occurs only at alternate dinucleotide steps of the type purine–purine (RR), pyrimidine–pyrimidine (YY) or pyrimidine–purine (YR) (except CG), both sugars change to $C_{3'}$-endo puckers, for RY steps the results are sequence dependent. In cases where the $\alpha\gamma$ flip occurs at all dinucleotide steps, alternating $C_{3'}$-endo and $C_{2'}$-endo sugars result, except in the case of CG. An example of such effects on the energy surface for dCG.rCG is shown in figure 6. It is finally remarked that $\alpha\beta\gamma$ flips were in general lost during surface calculations, the β dihedral easily reverted to its canonical value and this change lead to improved stability.

CONCLUSIONS

The molecular modelling carried out on DNA–RNA hybrids has shown that with virtually all homopolymeric and alternating sequences, the DNA strand adopts B-like $C_{2'}$-endo sugar puckers while the ribose strand always remains A-like with $C_{3'}$-endo sugars. The only exception to this rule involves the dT.rA hybrid duplex which was found to favour $C_{3'}$-endo puckers within the DNA strand, but was also shown to be able to pass to a B-like conformation with an energy difference of only 2.0 kcal/mol. This appears to be in line with the observed polymorphic behaviour of dT.rA under conditions of varying humidity, variations that we presently are unable to model explicitly. Our optimal hybrid conformations had canonical A/B-DNA backbone dihedrals ($\alpha\beta\gamma$: $g^-/t/g^+$) in agreement with recent experimental studies (9). These conformations have structural characteristics in between those of the usual A- and B- forms. In particular, they exhibit minor groove widths smaller than those of A-DNA duplexes, but larger than those in B-DNA. This finding is also in agreement with NMR studies of hybrids and has been used to explain the activity of RNase H towards these molecules (29). In contrast to Zimmerman and Pheiffer's fibre conformation (5) our findings do not support the existence of what we have termed an $\alpha\beta\gamma$ flip ($\alpha\beta\gamma$: $t/g^+/t$) within the DNA backbone. Inducing such a conformation in our case led to less stable structures and also led to a $B_{I \rightarrow B_{II}}$ backbone transition at low deoxyribose phase angles.

ACKNOWLEDGEMENTS

The authors wish to thank the Association for International Cancer Research (St Andrews University, UK) for their generous support of this project.

REFERENCES

1. Ogilvie, K.K., Usman, N., Nichoghosian, K. and Cedergren, R.J. (1988) Proc. Natl. Acad. Sci. (U.S.A.), 85, 5764–5768.
2. Usman, N. and Cedergren, R.J. (1992) Trends in Biological Sciences, 17, 334–339.
3. Milman, G., Langridge, R. and Chamberlin, M.J. (1966) Proc. Natl. Acad. Sci. (U.S.A.), 57, 1804–1810.
4. Gray, D.M. and Ratliff, R.L. (1975) Biopolymers, 14, 487–498.
5. Zimmerman, S.B. and Pheiffer, B.H. (1981) Nucleic Acids Res., 78, 78–82.
6. Shindo, H. and Matsumoto, U. (1984) J. Biol. Chem., 259, 8682–8684.
7. Arnott, S., Chandrasekaran, R., Millane, R.P. and Park, H.-S. (1986) J. Mol. Biol., 188, 631–640.
8. Chou, S.-H., Flynn, P. and Reid, B. (1989) Biochemistry, 28, 2435–2443.
9. Salazar, M., Fedoroff, O.Y., Miller, J.M., Ribeiro, S.N. and Reid, B.R. (1993) Biochemistry, 32, 4207–4215.
10. Poncin, M., Hartmann, B. and Lavery, R. (1992) J. Mol. Biol., 226, 775–794.
11. Poncin, M., Piazzola, D. and Lavery, R. (1992) Biopolymers, 32, 1077–1103.
12. Lavery, R. (1988) In 'Structure and Expression Vol 3. DNA Bending and Curvature' eds Olson, W.K., Sarma, R.H., Sarma, M.H. and Sundaralingam, M.. Adenine Press. pp191–211.
13. Lavery, R., Zakrzewska, K. and Pullman, A. (1984) J. Comp. Chem., 5, 363–373.
14. Lavery, R., Parker, I. and Kendrick, J. (1986) J. Biomol. Struct. Dynam., 4, 443–461.
15. Lavery, R., Sklenar, H., Zakrzewska, K. and Pullman, B. (1986) J. Biomol. Struct. Dynam., 3, 989–1014.
16. Altona, C. and Sundaraligam, M. (1972) J. Am. Chem. Soc., 94, 8205–8212.
17. Lavery, R. (1994) in Advances in Computational Biology Vol.1 JAI Press Inc, Connecticut USA. in press.
18. R. Lavery and B. Hartmann (1994) Biophys. Chem. in press.
19. Hingerty, B., Richie, R.H., Ferrel, T.L. and Turner, J.E. (1985) Biopolymers, 24, 427–439.
20. Zakrzewska, K., Poltev, V.I., Oguey, C. and Lavery, R., (1993) J. Mol. Struct. Theochem 286, 219–229.
21. Saenger, W. (1984) Principles of Nucleic Acid Structure. Springer-Verlag, New York.
22. Heinneman, U., Lauble, H., Frank, R. and Blöcker, H. (1987) Nucleic Acids Res., 15, 9531–9550.
23. Haran, T.E., Shakked, Z., Wang, A.H.-J. and Rich, A. (1987) J. Biomol. Struct. Dynam., 5, 199–217.
24. Privé, G.G., Heinemann, U., Chandrasekharan, S. Kan, L.S., Kopta, M.L. and Dickerson, R.E. (1987) Science, 238, 498–504.
25. Hartmann, B., Piazzola, D. and Lavery, R. (1993) Nucleic Acids Res., 21, 561–568.
26. Dock-Bregeon, A.C., Chevrier, B., Podjarny, A., Johnson, J., de Bear, J.S., Gough, G.R., Gilham, P.T. and Moras, D. (1989) J. Mol. Biol., 209, 459–474.
27. Rao, S.N. and Kollman, P. (1985) J. Am. Chem. Soc., 107, 1611–1617.
28. Vorlickova, M., Kypr, J. and Sklenar, V. (1983) J. Mol. Biol., 166, 85–92.
29. Fedoroff, O.Y., Salazar, M. and Reid, B.R. (1993) J. Mol. Biol. 233, 509–523.